

Figure S1

Fig. S1. GFP-Lmo7 co-expression rescues increased apical domain expansion in *lmo7* morphants

(A) Schematic diagram of the experimental design. *lmo7* ATG MO (30 ng) was injected into two ventral blastomeres of four-cell embryos (red). At 16-32 cell stage, RNA encoding control GFP (100 pg) or GFP-Lmo7 (100 pg) was injected into one of the ventral blastomeres (yellow). This sequential injection minimizes non-specific binding of morpholinos to RNA in the injection mixture. (B-B'') Representative image of the boundary between Lmo7MO cell clusters with Lmo7MO+GFP-Lmo7 cell clusters. Embryos were co-stained by phalloidin to outline the apical domain of individual cells. (C) Quantification of apical domain surface size. Control uninjected cells (n=96), *lmo7*-ATGMO+GFP cells (n=94) and *lmo7*-ATGMO+GFP-Lmo7 cells from more than five different embryos. Statistical significance of the difference between the median values was assessed by Dunn's test using a Bonferonni correction for the p-values. Scale bar: 10 μ m in B.

Figure S2

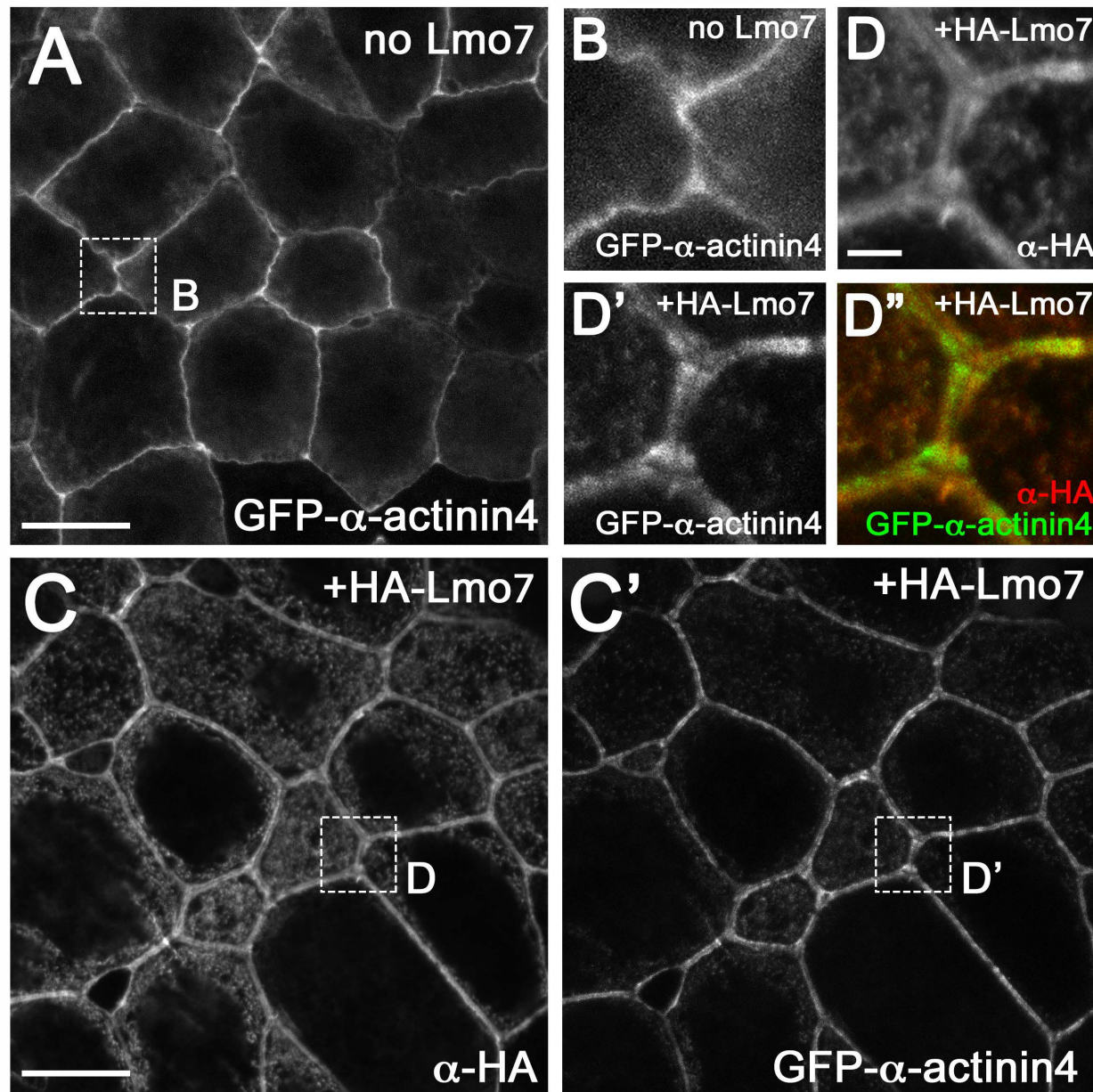


Fig. S2. Lmo7 promotes α -actinin enrichment in perijunctional actomyosin bundles RNA encoding GFP- α -actinin 4 (200 pg) was injected into 4-8 cell stage embryos with or without RNA encoding HA-Lmo7 (500 pg). (A, B) GFP- α -actinin 4 localizes at apical junctions and forms a single band. An area marked by a rectangle in A is enlarged in B. (C-D'') HA-Lmo7 promotes GFP- α -actinin 4 association with apical junctions. Areas marked by rectangles in C-C' are enlarged in D-D''. GFP- α -actinin 4 forms thick double bands that largely overlap HA-Lmo7. Scale bars: 10 μ m in A and C. 2 μ m in

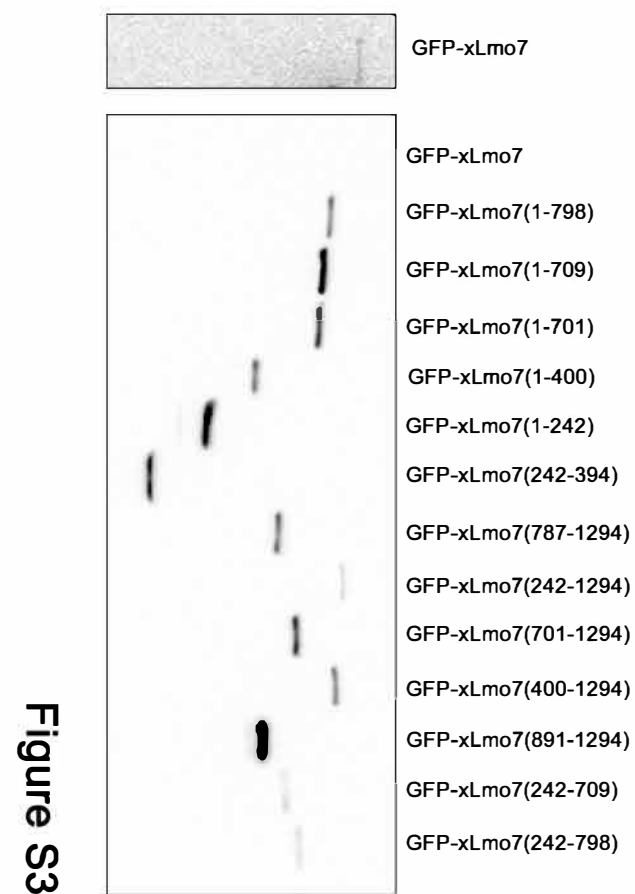


Fig. S3. Expression levels of GFP-Lmo7 constructs in *Xenopus* embryos

GFP-Lmo7 construct RNAs (1 ng) were injected into 4-8 cell stage embryos. Total embryo lysates were collected at stage 11. Expression levels of GFP-tagged Lmo7 constructs were assessed by immunoblotting with anti-GFP antibodies.

Long exposure of the sample from GFP-Lmo7-expressing embryos is shown on the left panel.

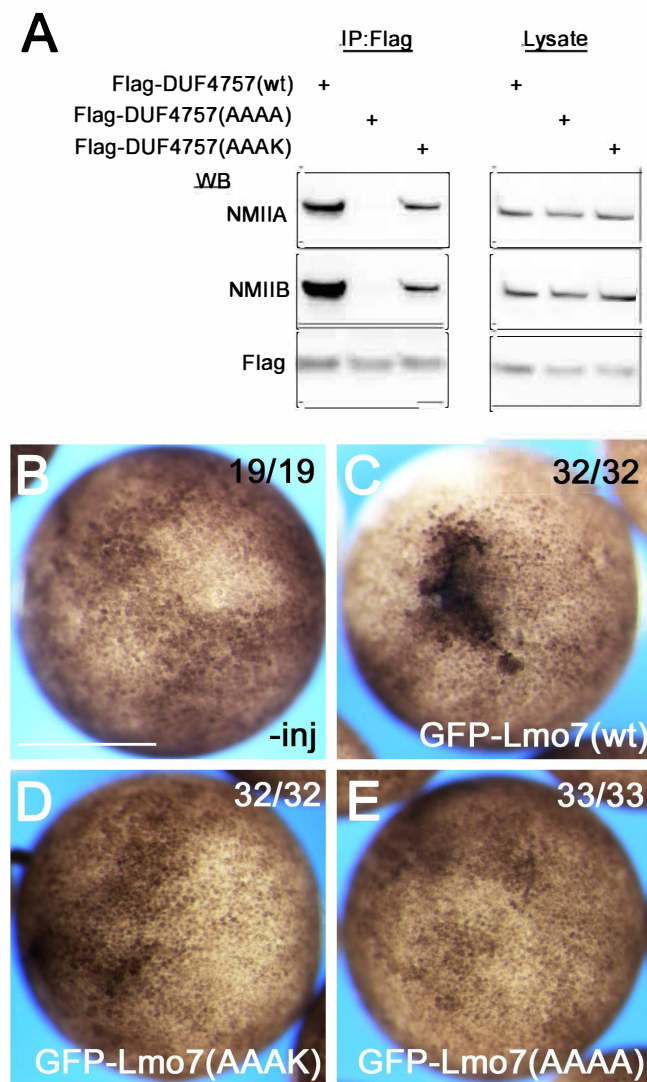


Figure S4

Fig. S4. The DUF4757 domain binds NMII heavy chains and is required for Lmo7-mediated apical constriction

(A) Flag-tagged DUF4757 (wt), DUF4757 (WQWK->AAAA), or DUF4757 (WQWK->AAAK) were transfected into HEK293T cells. Cell lysates were immunoprecipitated with anti-Flag antibody. Co-immunoprecipitation of endogenous NMIIA and NMIIB was examined by western blot. (B-E) Representative images of apical pigment granule accumulation in embryos expressing Lmo7 (wt), Lmo7(AAAK), and Lmo7(AAAA). Relevant RNA was injected into two blastomeres of 4-8 cell *Xenopus* embryos. Scale bar: 500 μ m in B.

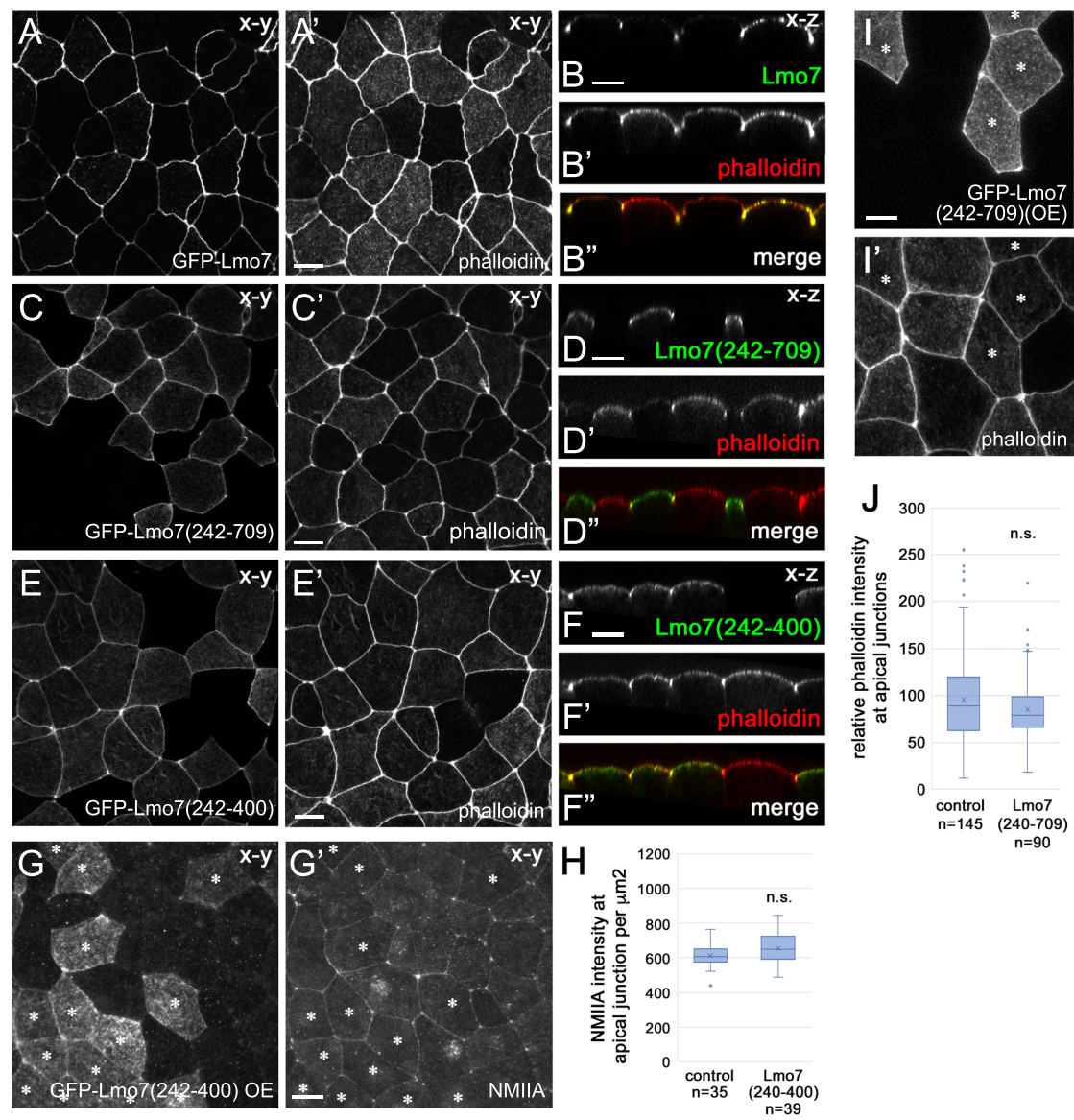


Figure S5

Fig. S5. The subcellular localization and effects of GFP-Lmo7(aa 242-709) on F-actin

RNAs were injected into 4-8 cell embryos. At stage 11, the embryos were fixed and the ectoderm was stained with phalloidin (A-F'', I-I'), or anti-GFP and NMIIA antibodies (G, G'). (A-F'') The subcellular localization of GFP-Lmo7 (A-B''), GFP-Lmo7(aa 242-709), and GFP-Lmo7(aa 242-400) after injection of 200 pg of each RNA. x-y view (A-A', C-C', E-E') and x-z view (B-B'', D-D'', F-F). Note that both Lmo7(aa 242-709)(C-D'') and Lmo7(aa 242-400) show more localization at the apical cortex, compared to full-length Lmo7. (G-H) The effects of GFP-Lmo7(aa 242-400)(1 ng RNA) on NMIIA in stage 11 ectoderm. (G-G') Ectodermal cells expressing GFP-Lmo7(aa 242-400)(asterisks). (H) Quantification of GFP-Lmo7(aa 242-400) effects on NMIIA at apical junctions. Fluorescent intensity of NMIIA was measured on individual cell-cell boundaries. (I-J) The effects of GFP-Lmo7(aa 242-709)(1 ng RNA) on F-actin in stage 11 ectoderm. (I, I') Ectodermal cells expressing GFP-Lmo7(aa 242-709)(asterisks). (J) Quantification of F-actin accumulation at apical junctions. Fluorescence intensity of phalloidin was measured at 3-10 locations within individual perijunctional F-actin bundles. Statistical significance of the difference between the median values was assessed by the Mann-Whitney U test. Data are representative of three independent experiments. Scale bar: 10 μ m.

Fig. S6. *Lmo7* expression in *Xenopus* embryos

(A) *Lmo7l* and *Lmo7s* expression was examined by RT-PCR. Both *Lmo7l* and *Lmo7s* are expressed maternally and zygotically throughout early embryonic development. (B-O) Expression of *Lmo7l* was examined by *in situ* hybridization. (B, D, F-N) *Lmo7l* antisense probes. (C, E, O) *Lmo7l* sense probes. Asterisks in B, C represent the blastopore. A: anterior. P: posterior. D: dorsal. V: ventral. nt: neural tube. pm: paraxial mesoderm. pe: preplacodal ectoderm. ht: heart. st: somites. pa: pharyngeal arches.

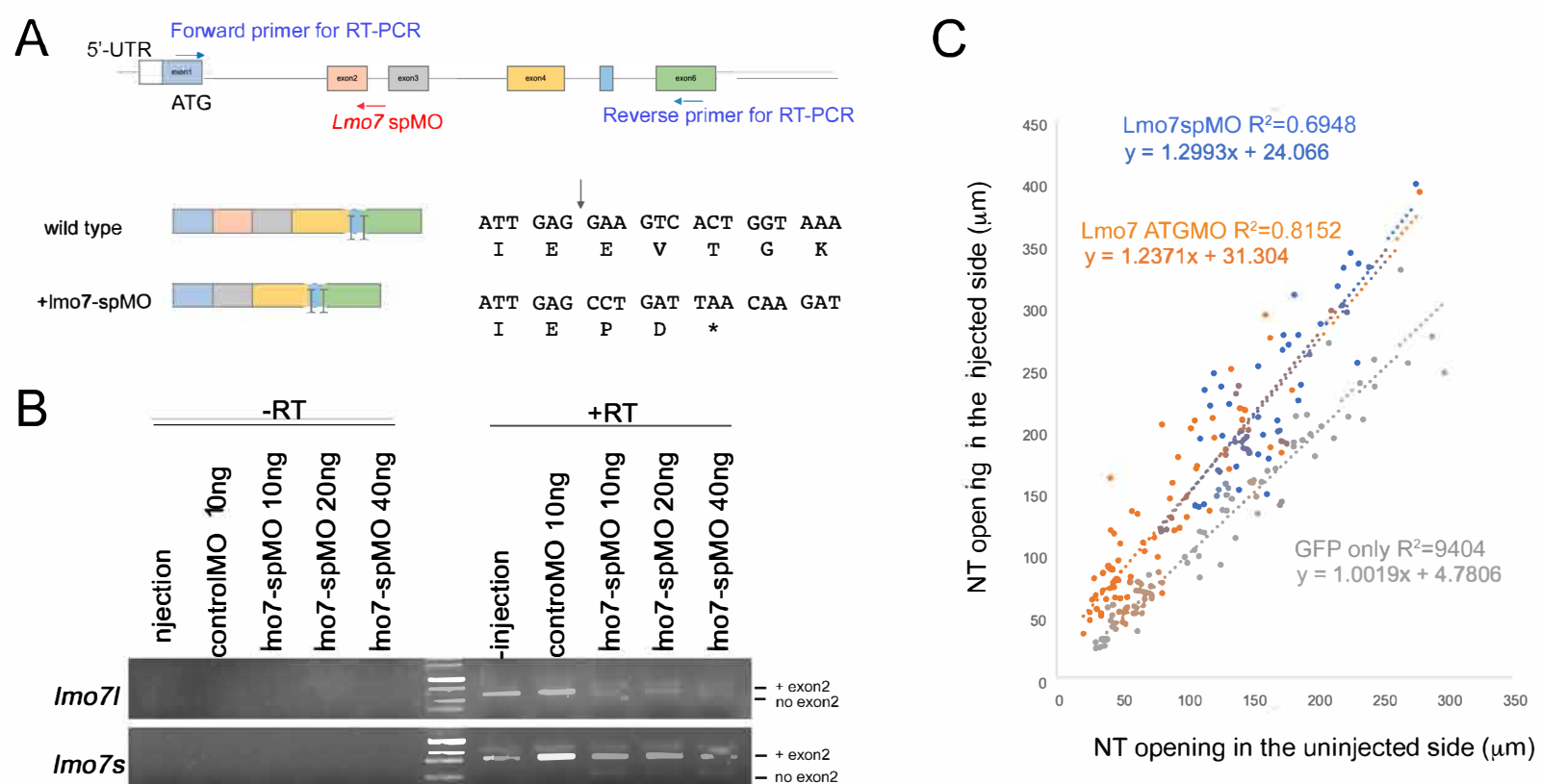


Figure S7

Fig. S7. Lmo7 knockdown delays neural tube closure

(A) Schematics of Lmo7 splicing blocking morpholino (Lmo7-spMO) design. Lmo7-spMO is designed to target the splicing donor site of exon 2. Lmo7-spMO sequence show 100 and 84% match to *Lmo7l* and *Lmo7s*, respectively. (B) RT-PCR results of *Lmo7l* and *Lmo7s* transcripts in *Lmo7-spMO* injected embryos. Note the appearance of lower bands. DNA sequencing of these bands confirmed the absence of the exon 2 and premature stop codon (shown in A). (C) Neural tube closure delay in Lmo7 knockdown embryos, related to Figure 9L. X-axis and Y-axis represent the widest distance from the midline to the edge of the neural fold in the control uninjected side and the injected side, respectively.

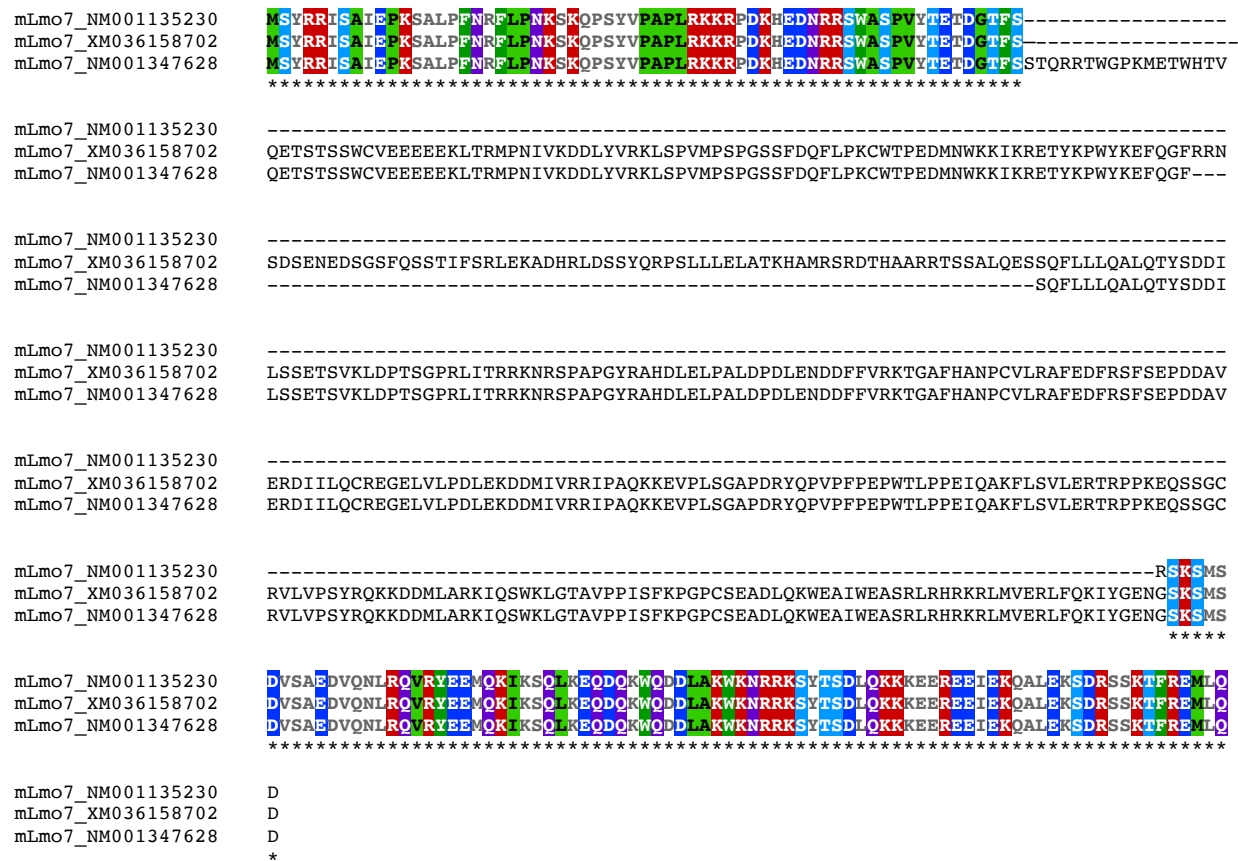
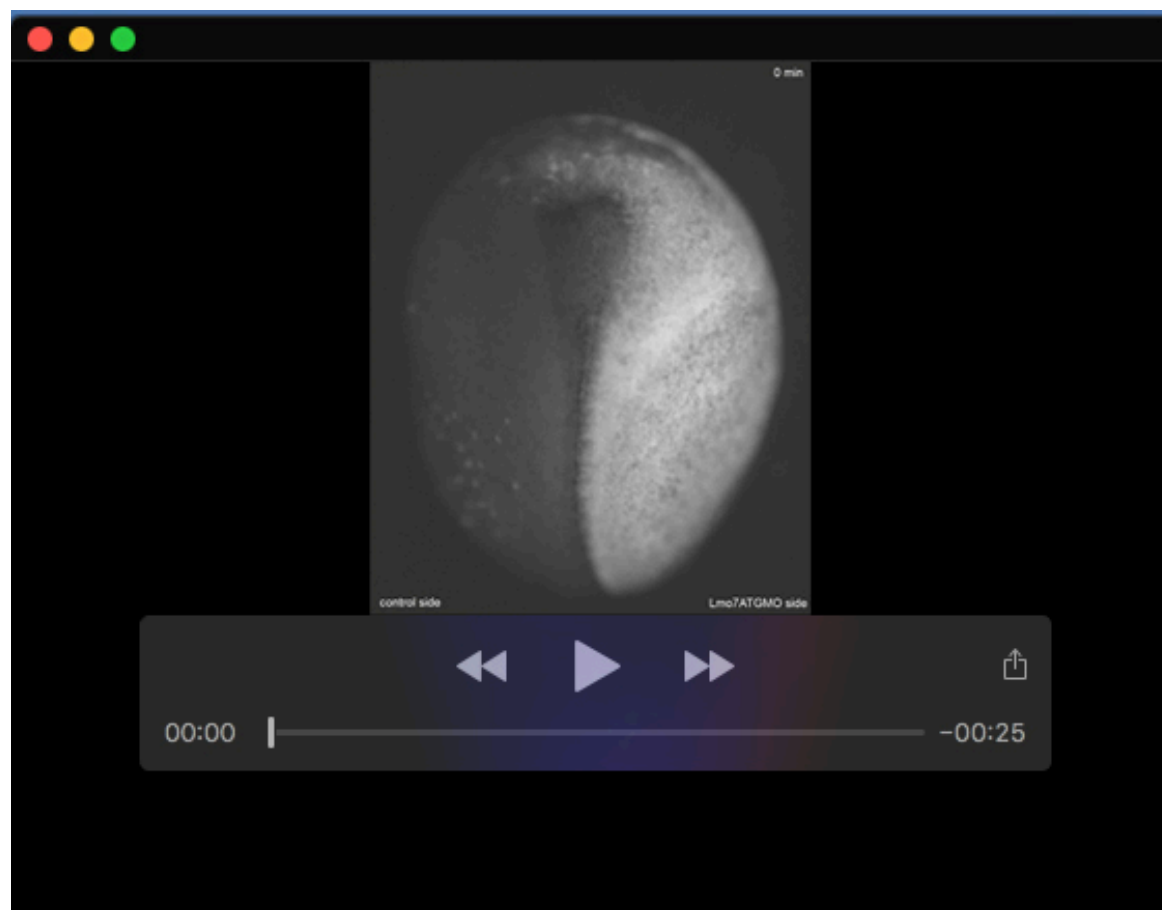


Fig. S8. Sequence alignment of DUF4757/NMIIBD among mouse Lmo7 splice variants

The DUF4757/NMIIBD were compared among three splice variants of *Mus musculus* Lmo7; NM_001135230, XM_036158702 and NM_001347628. Evolutionally conserved positively charged, negatively charged, hydrophobic and hydrophilic amino acids are marked by red, blue, green and purple as shown in Figure 7B. Conserved Ser/Thr are marked by light blue.

Table S1. Primer list

xLmo7-2F-EcoRI	gaattcgggaatggaatgaaaattc
xLmo7-242F-EcoRI	gaattccatgtcccatcgtagg
xLmo7-400F-EcoRI	gaattcggagagggaaacccg
xLmo7-700F-EcoRI	gaattcgtacagtgcctgagaat
xLmo7-787F-EcoRI	gaattctggcaagaatgactgg
xLmo7-898F-EcoRI	gaattcttgggatccagaaga
xLmo7-242R-stop-NheI	gctagctcagtcattcttctgctg
xLmo7-394R-stop-NheI	gctagctcaggtttccctctctgt
xLmo7-709R-stop-NheI	gctagctcaaggtttctggtaatgc
xLmo7-790R-stop-NheI	gctagctcagtcattcttgccatc
xLmo7-1028R-stop-NheI	gctagctcattttaaaacattattccttctg
xLmo7-1274R-stop-NheI	gctagctcacatggaggttg
xLmo7-WQWK(AAAA)-F	gagcaggatcagcagGCgGCgaatgatttagcaaaaGCgGCgaatcgtcgaaaaagc
xLmo7-WQWK(AAAA)-R	gctttttcgcagattcGCcGCttttgctaaatcattcGCcGCctgctgatcctgctc
morpholino	
xLmo7 ATGMO	GAATTTTCATTCATTCATTG
xLmo7 SpMO	AAATGCAAAGAATGTACTTACTCGC

**Movie 1. Lmo7 knockdown delays neural tube closure.**

Time-lapse recording of neural tube closure in embryos injected with Lmo7ATGMO only on the right side. GFP RNA is co-injected to trace the morpholino injected side. Dorsal view. Images were taken every 2 min. Duration of the time-lapse video is 176 min.